New BiOXs/TiO_2 heterojunction photocatalyst towards efficient degradation of organic pollutants under visible-light irradiation

Li Lun, Song Jinling ✉, *Wang Baoying, Duan Chenglin, Wang Ruifen, Zhang Bangwen*

School of Material and Metallurgy, Inner Mongolia University of Science and Technology, Baotou, Inner Mongolia 014010, People's Republic of China
✉ *E-mail: sjl2010004@imust.cn*

Published in Micro & Nano Letters; Received on 22nd September 2018; Revised on 24th February 2019; Accepted on 29th March 2019

A new heterojunction BiOXs/TiO_2 photocatalyst was firstly prepared by a mixed solvothermal method. Several tools were used to characterise the structure and morphologies of as-obtained samples. The results of photocatalytic experiments indicated that flower-like BiOXs/TiO_2 fabricated by the thinner nanosheets exhibited excellent degradation properties towards methyl orange, bisphenol A and tetracycline under visible-light irradiation. The reasons could be the good absorption of organic pollutants and light, and the high separation efficiency of photogenic electrons and holes attributed to the construction of BiOXs/TiO_2 heterojunction with large special surface areas. The photocatalytic mechanism was proposed. This Letter could provide new ideas to design the visible-light catalysts.

1. Introduction: Semiconductor photocatalytic technology has been considered as one of the most effective and green methods to solve the energy and environmental problems in human society [1–4], the key of which is the used photocatalysts [5–7]. However, the applications of TiO_2 traditional photocatalyst were seriously limited due to its large bandgap (3.2 eV) and further only absorption of UV irradiation ($\lambda < 390$ nm). For a new type of optical materials, bismuth oxyhalide (BiOX, X = Cl, Br, I) [8, 9], especially BiOX solid solutions have attracted extensive attention owing to their excellent visible photocatalytic properties [10]. Additionally, the construction of heterojunction has been proved to be an effective way to improve the photocatalytic activity [11–13]. As far as we know, there are abundant reports about BiOX/TiO_2 films and its applications on photocatalysis. However, the reported BiOX/TiO_2 materials were the composite materials of BiOX with one or two halogen elements and TiO_2 [14–19].

Herein, a new heterojunction photocatalyst between solid solutions of BiOXs with three halogen elements and TiO_2 was firstly in situ assembled by a mixed solvothermal method with the help of lactic acid. The photocatalytic degradation experiments indicate that BiOXs/TiO_2 can effectively decompose methyl orange (MO), bisphenol A (BPA) and tetracycline (TET) under the visible-light illumination. Moreover, the degradation efficiency is superior to that of the TiO_2 composite materials in the reported literature [20–28].

2. Experimental

2.1. Preparation: 6 mmol $Bi(NO_3)_3{\cdot}5H_2O$ was dissolved in 40 ml of glycol and 0.5 ml of lactic acid solution. In addition, 2 mmol NaCl, NaBr and NaI were simultaneously dissolved in a mixed solution contained 20 ml of ethanol and 20 ml of deionised water. Then, the above two solutions were further treated by sonic oscillation for 10 min and magnetically stirring for 30 min at room temperature. Thereinto, when the $Bi(NO_3)_3{\cdot}5H_2O$ solution was stirred up to 10 min, 1.0 ml tetrabutyl titanate were added to the solution and continued to stir for 20 min. After 30 min of stirring, the NaX solution was dropwise added to the $Bi(NO_3)_3{\cdot}5H_2O$ solution contained tetrabutyl titanate, which was kept stirring for another 30 min. Subsequently, the mixed solution was shifted to a 100 ml Teflon-lined stainless steel autoclave. The autoclave was placed in an oven for 12 h at 120°C. Finally, the obtained sample was centrifuged, washed and dried. The $BiOCl_{0.33}Br_{0.33}I_{0.33}/TiO_2$ photocatalyst was ground as a powder and labelled as BiOXs/TiO_2.

Besides, 6 mmol $Bi(NO_3)_3{\cdot}5H_2O$ was dissolved in 40 ml of glycol and 0.5 ml of lactic acid solution. Additionally, 2 mmol NaCl, NaBr and NaI were simultaneously dissolved in a mixed solution contained 20 ml of ethanol and 20 ml of deionised water. Then, the above two solutions were further treated by sonic oscillation for 10 min and magnetically stirring for 30 min at room temperature. After 30 min of stirring, the NaX solution was dropwise added to the $Bi(NO_3)_3{\cdot}5H_2O$ solution, which was kept stirring for another 30 min. The subsequent other steps were similar to the above mentioned process for BiOXs/TiO_2 synthesis. The corresponding product was BiOXs powder.

2.2. Characterisation: The X-ray diffraction (XRD) patterns of the as-prepared photocatalysts were recorded by a D8 advance (Bruker) diffractometer at CuKa radiation ($\lambda = 0.154618$ nm) with voltage 40 kV and current 40 mA. The field-emission scanning electron microscope (FE-SEM) analysis was conducted by a SU8220 (Hitachi) scanning electron microscope with an energy dispersive X-ray spectroscopy (EDS) for mapping the elemental. The X-ray photoelectron spectroscopy (XPS) was carried out in an ESCALAB 250Xi system. Quantachrome instruments Quadrasorb SI was used to measure the Brunauer–Emmett–Teller (BET) surface areas of the samples at 77.3 K.

2.3. Photocatalytic activity: The photocatalytic activities of the prepared samples were assessed by the degradation of MO (20 mg/l), BPA (15 mg/l) and TET (30 mg/l) under the visible light. The light source was a xenon lamp (300 W, PLX-SXE 300UV, Beijing Perfect Light Technology Co. Ltd.), which was outfitted a 400 nm cut-off filter. For the photodegradation experiment, 20 mg photocatalyst was dispersed in 100 ml solution. The mixture was stirred for 30 min to reach an adsorption–desorption equilibrium in the dark. The removal rate of organic pollutant was monitored by measuring the changes at its maximum absorption wavelength with a UV–vis spectrophotometer every 30 min. The photocatalytic efficiency is calculated by η using the Lambert–Beer law [29, 30]. $\eta = C/C_0 = A/A_0$, where the C is the reaction concentration and C_0 is the initial concentration. A and A_0 are the equivalent absorbencies. Meanwhile, the commercial P_{25} (Evonik Deguss) is used as a reference sample to estimate the photo-activity of the prepared samples.

3. Results and discussion

3.1. Characterisation: For BiOX, it is well known that two major crystal planes of (110) and (102) matched with the $[Bi_2O_2]^{2+}$ and X^- slabs structure, respectively [15]. The difference of halogen ions radius makes the corresponding crystalline interplanar spacing and the diffraction angles different. The smaller radius of halogen ion makes the corresponding diffraction angles shift towards higher-angle. Fig. 1 shows the XRD patterns of the as-prepared BiOXs and BiOXs /TiO_2 powders. As shown in the inset of Fig. 1, the (110) and (102) diffraction peaks of as-prepared BiOXs are at 32.286° and 31.298°, respectively, which are between the standard BiOCl (JCPDS Card No. 06-0249) and BiOI (JCPDS Card No. 10-0445), and close to standard BiOBr (JCPDS Card No. 09-0393/52-0084). The gradual shift of the XRD pattern indicates that the BiOXs is a solid solution [31, 32]. In addition, the XRD pattern of BiOXs/TiO_2 heterojunction is similar to that of BiOXs, implying that the addition of TiO_2 does not destroy the structure of BiOXs.

As shown in Figs. 2*a* and *d*, the morphologies of as-prepared BiOXs and BiOXs/TiO_2 samples were all irregular 3D flowerlike nanoparticles with stratified structure. For BiOXs sample, the diameter of the microspheres is about 0.6–2.0 µm, whose lamella thickness is 10–50 nm. For BiOXs/TiO_2 sample, the diameters of irregular spheres are in the range of 0.4–1.5 µm, having radially grown nanoplates about 5–20 nm. The thicknesses of BiOXs/TiO_2 plates are thinner than that of BiOXs. The results could induce the difference on the specific surface areas of the two samples. The specific surface area of BiOXs sample is only 37.181 m^2/g. In comparison, the specific surface area of BiOXs/TiO_2 sample obtains 93.566 m^2/g. Moreover, the EDS and elemental mappings were used to define the composition of these samples. The measurement results of the BiOXs sample show that the sharp peaks of Bi, O, Cl, Br and I elements appear in the corresponding energy positions (Fig. 2*b*) and equally distributed in element mappings (Fig. 2*c*). Similar to the BiOXs, the elements of Bi, Cl, Br and I could be also detected for the BiOXs/TiO_2 sample, as shown in Fig. 2*e*. In addition, a peak of titanium was discovered. The element mappings (Fig. 2*f*) show that the titanium element is also very well distributed.

To further define the surface chemical bonding of BiOXs/TiO_2 sample, XPS analysis was carried out and the corresponding results (Fig. 3*a*) indicated that the heterojunction consisted of Bi, O, Cl, Br, I and Ti elements except for a carbon contamination signal at 284.8 eV. The high-resolution XPS of Ti 2p in Fig. 3*b* with two peaks at 458.9 and 466.5 eV could be deconvoluted into $2p_{3/2}$ and $2p_{1/2}$, offering the guarantee of Ti^{4+} in the composite [17]. Based on those results, the new BiOXs/TiO_2 heterojunctions with high surface areas have been synthesised by the mixed solvothermal method.

3.2. Photocatalytic activity and mechanism: MO (20 mg/l), BPA (15 mg/l) and TET (30 mg/l) with different structures were selected to evaluate the photocatalytic activity of the prepared samples. As shown in Fig. 4, the synthesised BiOXs/TiO_2 exhibits the most excellent photocatalytic activity among the prepared samples and P_{25}. Under visible-light illumination for 180 min, the degradation efficiency for MO, BPA and TET obtain 93, 72 and 90%, respectively. From the detailed absorption spectra of the

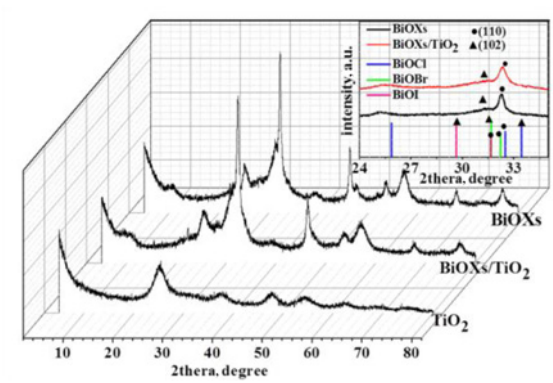

Fig. 1 *XRD patterns of the prepared samples*

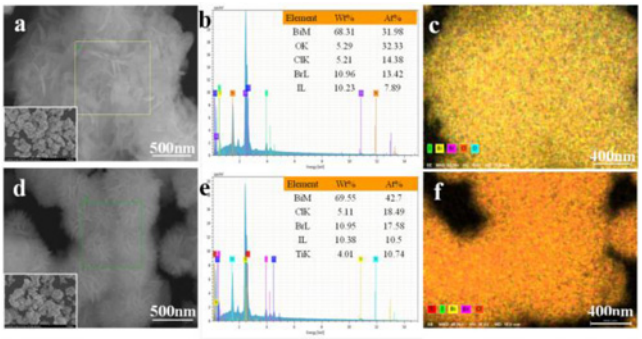

Fig. 2 *FE-SEM*
a–c EDS and elemental mapping of BiOXs
d–f BiOXs/TiO_2

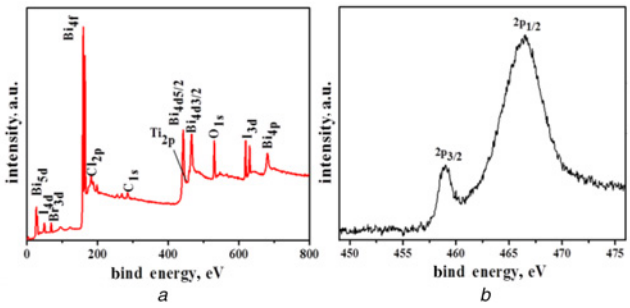

Fig. 3 *XPS of BiOXs/TiO_2 photocatalyst*
a Survey scan
b Ti 2p spectra

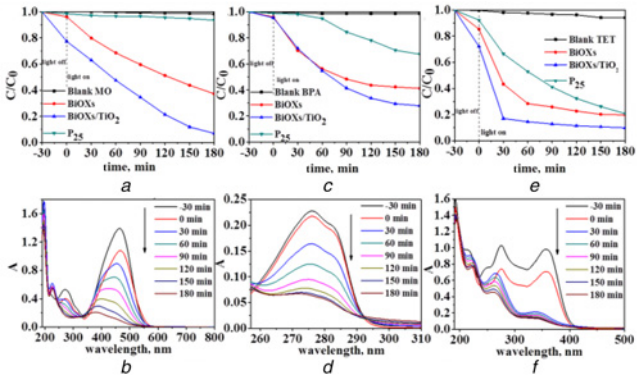

Fig. 4 *Photocatalytic degradation curves of organic pollutant over the as-prepared photocatalysts and P_{25}*
a MO
c BPA and
e TET. The temporal adsorption spectra of organic pollutants in the presence of the as-prepared BiOXs/TiO_2
b MO
d BPA and
f TET

doi: 10.1049/mnl.2018.5584

Table 1 Comparison the photocatalytic activities of TiO_2 composite catalysts

Photocatalysts	Target pollutant	Light source	Time $\eta_{degradation}$	TOF[a] (10^{-2} g/g·min)	Ref.
BiOI-TiO_2 (0.1 g)	BPA (20 mg/l)	250 W Xe lamp 400 nm cut off	90 min (55%)	0.024	[20]
BiOI-TiO_2 (0.05 g)	MO (20 mg/l)	350 W Xe lamp 410 nm cut off	120 min (98.2%)	0.016	[21]
N-TiO_2/rGO (0.05 g)	TET (10 mg/l)	300 W Xe lamp 400 nm cut off	60 min (98%)	0.016	[22]
CdS/TiO_2 (0.05 g)	MO (10 mg/l)	300 W Xe lamp 463 nm cut off	70 min (100%)	0.014	[23]
$MnFe_2O_4$/g-C_3N_4/TiO_2 (0.5 g/l)	MO (10 mg/l)	150 W Xe lamp	180 min (99.3%)	0.011	[24]
g-C_3N_4/TiO_2-74.4 (0.4 g)	MO (5 mg/l)	350 W Xe lamp	80 min (80%)	0.005	[25]
TiO_2-g-C_3N_4(0.06 g)	MO (10 mg/l)	300 W Xe lamp	180 min (80%)	0.004	[26]
g-C_3N_4/Gd-N-TiO_2 (0.08 g)	MB (10 mg/l)	350 W Xe lamp 420 nm cut off	180 min (98%)	0.012	[27]
SnO_2/ZnO/TiO_2 (0.15 g)	MO (10 ppm)	300 W Xe lamp 400 nm cut off	240 min (77%)	0.003	[28]
BiOXs/TiO_2 (0.020 g)	MO (20 mg/l) BPA (15 mg/l) TET (20 mg/l)	300 W Xe lamp 400 nm cut off	180 min (93, 72, 90%)	0.052, 0.030, 0.050	this work

[a]TOF(Turnover frequency) $= \dfrac{C_{\text{target pollution}} \times V_{\text{target pollution}} \times \eta_{\text{degradation}}}{m_{\text{photocatalyst}} \times t_{\text{degradation}}}$.

BiOXs/TiO_2 (Figs. 4*b*, *d* and *f*), the absorption band intensities of organic pollutants always decrease with the increasing of irradiation time, implying the organic pollutants could be effectively degraded during the photo illumination process. In addition, compared with other reported TiO_2 composite catalysts (Table 1), BiOXs/TiO_2 also displays excellent photocatalytic activity [20–28].

The recycling test investigated the photocatalyic stability of the BiOXs/TiO2 catalyst. After four recycles, the MO degradation rate can be maintained at about 88%, implying the good stability of BiOXs/TiO_2. A slight decrease in photocatalytic activity after four cycles could be mainly attributed to the loss of catalyst during washing and recycling processes.

The photocatalytic mechanism of BiOXs/TiO_2 should proceed in the P–N junction heterostructure mechanism [33–35]. For the heterojunction, the electrons in the valence band (VB) of the BiOXs can be excited to the conduction band (CB) under visible light illumination, leaving holes (h^+) in the VB. Then, a part of the electrons can transfer to the CB of TiO_2, and meanwhile another part of the electrons reduce the dissolved oxygen in aqueous solution to produce active superoxide radical ($\bullet O_2^-$). The $\bullet O_2^-$ radicals react with the adsorbed organic pollutions, and a little bit of it further reacts with hydrogen ions (H^+) to form active hydroxyl radicals ($\bullet$OH). Finally, all the holes leaved in the VB of BiOXs. These produced active species ($\bullet O_2^-$, $\bullet$OH and h^+) can directly react with the organic pollution to produce degradation products. The construction of BiOXs/TiO_2 and the presence of large surface areas are favourable to separate the photo-generated electron–hole pairs, absorb pollutants and harvest light, which are the main factors for the promotion of photocatalytic activity.

4. Conclusion: Flower-like BiOXs solid solution and TiO_2 heterojunction assembled with thinner nanosheets have been prepared through the solvothermal method. The photocatalytic experimental results show that the heterojunction exhibit more excellent photocatalytic properties than BiOXs and P_{25} under visible light irradiation towards MO, BPA and TET solutions. The reasons can be attributed to the construction of BiOXs/TiO_2 and the presence of large surface area, which can improve the absorption of organic pollutants and light, and the high separation efficiency of photogenic electrons and holes. The findings could provide an idea for the development of the later composite catalysts in the photocatalytic field.

5. Acknowledgments: This work was support by the Natural Science Foundation of China (grant no. 21407084), the In-novation Foundation of Inner Mongolia University of Science and Technology (grant no. 2018YQL01), and the Natural Science Foundation of Inner Mongolia (grant nos. 2014BS0509, 2015MS0571, 2017BS0508).

6 References

[1] Regulacio M.D: 'Multinary I-III-VI2 and I2-II-IV-VI4 semiconductor nanostructures for photocatalytic applications', *Accounts Chem. Res.*, 2016, **49**, (3), pp. 511–519
[2] Abdullah M.A: 'Tin dioxide as a photocatalyst for water treatment: a review', *Process. Saf. Environ.*, 2017, **107**, pp. 190–205
[3] X, Li: 'Hierarchical photocatalysts', *Chem. Soc. Rev.*, 2016, **45**, (9), pp. 2603–2636
[4] Feng L.Y: 'Enhanced photocatalytic H2-production activity of C-dots modified g-C_3N_4/TiO_2 nanosheets composites', *J. Colloid Interface Sci.*, 2018, **513**, pp. 866–876
[5] Long X.Z: 'Enhanced photocatalysis of g-C_3N_4 thermally modified with calcium chloride', *Catal. Lett.*, 2017, **147**, (8), pp. 1922–1930
[6] Mamba G: 'Graphitic carbon nitride (g-C_3N_4) nanocomposites: a new and exciting generation of visible light driven photocatalysts for environmental pollution remediation', *Appl. Catal. B Environ.*, 2016, **198**, pp. 347–377
[7] Li Q W: 'Green photocatalysis with oxygen sensitive BODIPYs under visible light', *Catal. Lett.*, 2014, **144**, (2), pp. 308–313
[8] Jiang S.H: 'Facile synthesis of a rose-like BiOCl assembled from nanosheets and its thermal-property application in polymers', *Mater. Lett.*, 2015, **161**, pp. 561–564
[9] Cheng H: 'Engineering BiOX (X = Cl, Br, I) nanostructures for highly efficient photocatalytic applications', *Nanoscale*, 2014, **6**, pp. 2009–2026
[10] Wu T.L: 'Efficient visible light photocatalytic oxidation of NO with hierarchical nanostructured 3D flower-like $BiOCl_xBr_{1-x}$ solid solutions', *J. Alloys Compd.*, 2016, **671**, pp. 318–327
[11] Zhang L: 'Toward designing semiconductor-semiconductor heterojunctions for photocatalytic applications', *Appl. Surf. Sci.*, 2017, **430**, pp. 2–17
[12] Zhu Z.J: 'A novel p-n heterojunction of $BiVO_4$/TiO_2/GO composite for enhanced visible-light-driven photocatalytic activity', *Mater. Lett.*, 2017, **209**, pp. 379–383
[13] Wang L.: 'Daoud, BiOI/TiO_2-nanorod array heterojunction solar cell: growth, charge transport kinetics and photoelectrochemical properties', *Appl. Surf. Sci.*, 2015, **324**, pp. 532–537
[14] Odling G: 'SILAR BiOI-sensitized TiO_2, films for visible-light photocatalytic degradation of rhodamine B and 4-chlorophenol', *Chem. Phys. Chem.*, 2017, **18**, (7), pp. 728–735
[15] Yang J: 'Preparation and photocatalytic activity of BiOX–TiO_2 composite films (X = Cl, Br, I)', *Ceram. Int.*, 2014, **40**, (6), pp. 8607–8611
[16] Li L: 'Hierarchical assembly of BiOCl nanosheets onto bicrystalline TiO_2 nanofiber: enhanced photocatalytic activity based on photoinduced interfacial charge transfer', *J. Colloid Interface Sci.*, 2014, **435**, pp. 26–33
[17] Wu D: 'Photocatalytic self-cleaning properties of cotton fabrics functionalized with p-BiOI/n-TiO_2 heterojunction', *Surf. Coat. Technol.*, 2014, **258**, pp. 672–676

[18] Cai Y: 'Grafting BiOCl nanosheets onto TiO_2 tubular arrays to form a hierarchical structure with improved photocatalytic performance', *RSC Adv.*, 2013, **3**, (41), pp. 19064–19069
[19] Dalia S.R: 'Photocatalytic properties of BiOCl-TiO_2 composites for phenol photodegradation', *J. Environ. Chem. Eng.*, 2018, **6**, (2), pp. 1601–1612
[20] Chen Y: 'Synthesis of BiOI-TiO_2 composite nanoparticles by micro-emulsion method and study on their photocatalytic activities', *Scientific World J.*, 2014, **5**, pp. 1–8
[21] Li Z: 'Synthesis of BiOI nanosheet/coarsened TiO_2 nanobelt hetero-structures for enhancing visible light photocatalytic activity', *RSC Adv.*, 2016, **6**, pp. 30037–30047
[22] Tang X: 'Visible active N-doped TiO_2/reduced graphene oxide for the degradation of tetracycline hydrochloride', *Chem. Phys. Lett.*, 2018, **691**, pp. 408–414
[23] Zhou P.P: 'Studies on facile synthesis and properties of mesoporous CdS/TiO_2 composite for photocatalysis applications', *J. Alloys Compd.*, 2017, **692**, pp. 170–177
[24] Vignesh K: 'Photocatalytic activity of magnetically recoverable $MnFe_2O_4$/g-C_3N_4/TiO_2 nanocomposite under simulated solarlight irradiation', *J. Mol. Catal. A, Chem.*, 2014, **395**, 373–383
[25] Li J.H: 'Fabrication of g-C_3N_4/TiO_2 composite photocatalyst with extended absorption wavelength range and enhanced photocatalytic performance', *J. Photochem. Photobiol. A*, 2016, **317**, pp. 151–160
[26] Zhang B: 'Molten salt assisted in-situ synthesis of TiO_2/g-C_3N_4 composites with enhanced visible-light-driven photocatalytic activity and adsorption ability', *J. Photochem. Photobiol. A*, 2018, **362**, pp. 1–3
[27] Yu Y.M: 'Exceedingly high photocatalytic activity of g-C_3N_4/Gd-N-TiO_2 composite with nanoscale heterojunctions', *Sol. Energy Mater. Sol. Cells*, 2017, **168**, pp. 91–99
[28] Yang G.D: 'Preparation and characterization of SnO_2/ZnO/TiO_2 composite semiconductor with enhanced photocatalytic activity', *Appl. Surf. Sci.*, 2012, **258**, pp. 8704–8712
[29] Aghdam S.M: 'Precipitation dispersion of various ratios of BiOI/BiOCl nanocomposite over g-C_3N_4 for promoted visible light nano-photocatalyst used in removal of acid orange 7 from water', *J. Photochem. Photobiol. A*, 2017, **338**, pp. 201–212
[30] Zhang J.F: 'Design of a direct Z-scheme photocatalyst: preparation and characterization of Bi_2O_3/g-C_3N_4 with high visible light activity', *J. Hazard. Mater.*, 2014, **280**, pp. 713–722
[31] Kim W.J: 'Adsorption/photocatalytic activity and fundamental natures of BiOCl and $BiOCl_xI_{1-x}$ prepared in water and ethylene glycol environments, and Ag and Au-doping effects', *Appl. Catal. B Environ.*, 2014, **147**, pp. 711–725
[32] Liu Y.Y: 'Composition dependence of the photocatalytic activities of $BiOCl_{1-x}Br_x$ solid solutions under visible light'. *J. Chem. Eur.*, 2011, **17**, pp. 9342–9349
[33] Wang L: 'BiOI/TiO_2-nanorod array heterojunction solar cell: growth, charge transport kinetics and photoelectrochemical properties', *Appl. Surf. Sci.*, 2015, **324**, pp. 532–537
[34] Wang X.J: 'Construction of amorphous TiO_2/BiOBr heterojunctions via facets coupling for enhanced photocatalytic activity', *Hazardous Mater.*, 2015, **292**, pp. 126–136
[35] Liu X.Y: 'A heterojunction Cu_2O/N–TiO_2 photocatalyst for highly efficient visible light-driven hydrogen production', *Catal. Lett.*, 2016, **146**, (9), pp. 1655–1662

doi: 10.1049/mnl.2018.5584